Organic Electronics 13 (2012) 309–319

Contents lists available at SciVerse ScienceDirect

Organic Electronics

journal homepage: www.elsevier.com/locate/orgel

Interface electronic structure between organic semiconductor film and electrode metal probed by photoelectron yield spectroscopy

Kaname Kanai [a,*], Masato Honda [b], Hisao Ishii [c], Yukio Ouchi [b], Kazuhiko Seki [b]

[a] Department of Physics, Tokyo University of Science, 2641 Yamazaki, Noda-shi, Chiba 278-8510, Japan
[b] Graduate School of Science, Nagoya University, Furo-cho, Chikusa-ku, Nagoya 464-8602, Japan
[c] Center for Frontier Science, Chiba University, 1-33, Yayoi-cho, Inage-ku, Chiba-shi, Chiba 263-8522, Japan

ARTICLE INFO

Article history:
Received 20 October 2011
Received in revised form 21 November 2011
Accepted 25 November 2011
Available online 13 December 2011

Keywords:
Interface electronic structure
Organic semiconductor film
Photoelectron yield spectroscopy

ABSTRACT

We present an investigation of the interface between organic semiconductor films and metal substrates (organic/metal interface) using photoelectron yield spectroscopy (PYS) as the probing technique. PYS studies were conducted on the pentacene/Au, copper phthalocyanine (CuPc)/Au, and perfluorinated zinc phthalocyanine (F_{16}ZnPc)/Au, and the results were compared with literature results obtained using conventional ultraviolet photoemission spectroscopy (UPS). PYS is advantageous for probing the electronic structure of the organic/metal interface because of the relatively long mean free path of photoexcited electrons with very low kinetic energy in PYS, which enables the detection of the photoelectrons from the metal substrate buried deep in the organic film. We demonstrate herein that the use of PYS reduces the significance of the final state effect of the electronic density surrounding the photohole at the organic molecule generated after the photoemission; this effect is known as the electric polarization effect. Although this effect has a significant influence on the results obtained using conventional UPS, the reduced influence of the final state effect in PYS makes it possible to construct an energy level diagram at the organic/metal interface with greater accuracy than can be achieved with UPS. In addition, a novel mechanism of the photoelectron detection for PYS enables us to apply PYS to very thick organic films, and therefore, PYS provides a reliable value of ionization energy for organic films without the influence of the substrate.

Because the interface electronic structure has a significant influence on the carrier injection properties of organic devices, the increased reliability of the information obtained by PYS will render it very useful for the improvement of device performance as well for understanding their operation principles.

1. Introduction

The elucidation of the electronic structure of the interface between organic semiconductor films and electrode metals (organic/metal interface) is one of the key issues in the field of basic research on organic electronics. The performance of organic optical and electronic devices such as light emitting diodes (OLEDs) or field effect transistors (OFETs) is strongly influenced by the efficiency of the carrier injection across the organic/metal interface. Consequently, an understanding of the factors affecting the carrier injection barrier at the organic/metal interface is crucial for improved device performance. In pioneering studies by Ishii et al., it was reported that the electric double layer (Δ) formed within a few molecular layers directly on the electrode metal surface upon the injection barrier has a profound impact on the carrier injection barrier [1,2]. Although many theoretical and experimental

* Corresponding author. Tel.: +81 4 7122 1481; fax: +81 4 7123 9361.
E-mail address: kaname@ph.noda.tus.ac.jp (K. Kanai).

1566-1199/$ - see front matter © 2011 Elsevier B.V. All rights reserved.
doi:10.1016/j.orgel.2011.11.024

investigations have been executed in an attempt to understand the origin of Δ [3–11], the question remains unresolved. Ultraviolet photoemission spectroscopy (UPS), which is a powerful tool for directly probing the occupied interface electronic structure, has played an important role in the research on organic/metal interfaces. For example, some researchers have adopted the thickness dependence of the UPS spectra for the organic film deposited on a metal surface as a standard technique for describing the energy level diagram at the organic/metal interface [12–15]. The energy level diagram of the organic/metal interface can be obtained by plotting the vacuum level energy and molecular orbital energies, which are derived from an analysis of the UPS spectra for different organic film thicknesses. Nonetheless, it should be noted that UPS is not always a satisfactory method for investigating the electronic structure at the organic/metal interface given that UPS is a very surface sensitive technique because of its quite short probing depth, which is less than 0.5 nm in the ultraviolet or vacuum ultraviolet region [16]. UPS probes the outermost surface regions of the organic film. However, in practical organic devices, the organic/metal interface is buried deep inside the organic layers. Thus, UPS cannot be used to probe this "buried interface" directly, and the interface electronic structure derived from the thickness dependence of the UPS spectra provides only an approximate picture of the organic/metal interface. It is known that when an organic molecule is suddenly ionized by photoexcitation, some relaxations of the ionized molecule, including reactions of its surroundings, occur immediately. As a result, UPS spectra are always accompanied by the characteristic final state effects that arise mainly from the relaxation of the photohole created at the organic molecule following photoemission, and such effects sometimes prevent us from getting a true picture of the organic/metal interface [17–20]. A careful examination of the organic/metal interface via direct observation with other complementary technique is thus necessary in order to obtain a correct understanding of the organic/metal interface from both qualitative and quantitative viewpoints.

In this study, photoelectron yield spectroscopy (PYS) was employed as a means of direct observation of the organic/metal interface. In PYS, photoelectrons emitted from the sample are collected by varying the excitation photon energy ($h\nu$) from the visible to the ultraviolet energy region [21,22]. One of the noteworthy advantages of PYS is its very long probing depth. It is known that the escape depth of a photoelectron increases dramatically as its kinetic energy (E_k) decreases from several tenths of electron volts due to the reduction in the electron–electron scattering rate inside the solid [16]. PYS measurements were performed herein by sweeping $h\nu$, typically from 3 to 6 eV. Photoelectrons excited by such low energy photons have a mean free path that may be as large as 10 nm, and therefore, photoelectrons from the buried interface can escape from the sample surface. The mean free path of electrons is defined as the characteristic distance where the amount of photoelectrons decreases to e^{-1} times its initial amount as the photoelectrons travel inside the solid, where e is a natural logarithm base. This means that theoretically, at a mean free path of 10 nm for the photoelectron, 14% of the photoelectrons from the metal surface buried under a 20 nm thick organic film can still escape from the sample surface as photoelectrons. As will be expounded in detail later in the text, this study illustrates that photoemission from a metal substrate covered with a 50 nm thick organic film can be clearly observed in the PYS spectra. The principle of PYS used to investigate the organic/metal interface is illustrated in Figs. 1 and 2. During PYS measurement, the sample is initially irradiated using monochromatic light with tunable photon energy ($h\nu$); photoelectrons are then emitted from the sample surface. The total number of photoelectrons, i.e., the sum of the direct and secondary photoelectrons per incident photon (photoelectron yield, Y), is counted as a function of $h\nu$. The photoemission process is schematically represented in Fig. 1. The photoemission process can be divided into three steps as follows: (1) photoexcitation of the electron by the incident photons occurs at the metal or the organic film, (2) the excited electrons travel toward the surface and produce a number of secondary electrons with a certain probability, and (3) the excited electrons and secondary electrons penetrate through the surface into the vacuum as photoelectrons. In general, the minimum $h\nu$ required to generate a photoelectron from the metal differs from that required to generate a photoelectron from the organic film. In Fig. 1, the photoelectrons from the metal and organic films are labeled "A" and "B," respectively. Fig. 2a shows the energy level diagram for the photoemission process presented in Fig. 1. The photoelectrons from the metal (labeled A in Fig. 1) can escape from the surface to the vacuum when $h\nu_A$ is higher than ε^F_{vac}. Here, ε^F_{vac} represents the energy interval between Fermi level (E_F) of the metal and vacuum level of the sample. On the other hand, the photoelectrons from the organic film (labeled B) can escape from the surface to the vacuum when $h\nu_B$ becomes higher than I. Here, I represents the ionization energy of the organic film, which is defined as the energy interval between the vacuum level and the highest occupied molecular orbital (HOMO) energy of the organic film. In general, as depicted in Fig. 2a, $h\nu_B$ is higher than $h\nu_A$ by E_{HOMO}. E_{HOMO} represents the HOMO energy with respect to E_F. Fig. 2b presents the schematic PYS spectrum for an organic/metal interface corresponding to the process shown in Fig. 2a. The photoelectron yield (Y) is plotted to the $1/n$ power as a function of $h\nu$. The PYS

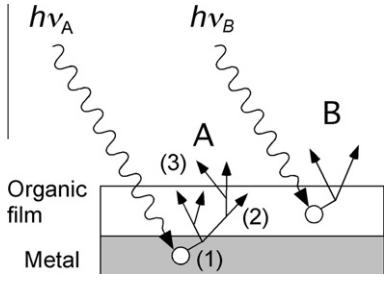

Fig. 1. Schematic drawing of photoemission from metal substrate (A) and organic film (B). The numbers represent the following processes: (1) photoexcitation of the electron, (2) transport of the excited electrons to the surface, and (3) penetration of the electrons through the surface into the vacuum, respectively.

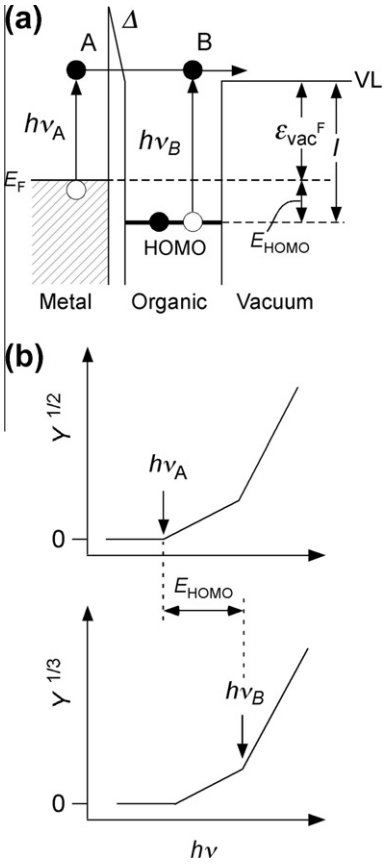

Fig. 2. (a) Schematic energy level diagram for photoemission process depicted in Fig. 1. (b) Schematic PYS spectrum for organic/metal interface. The ordinate represents the photoelectron yield, $Y^{1/n}$ (where $n = 2, 3$) and the abscissa represents the excitation photon energy, $h\nu$.

spectrum around the photoelectric threshold is usually expressed by the relation, $Y^{1/n} \propto (h\nu - h\nu^{th})$, where $h\nu^{th}$ represents the threshold energy for the photoemission and n is a parameter that mainly depends on the shape of the density of electronic states at the upper edge of the occupied states and the transmission probability of electrons across the sample surface [23–26]. The square-root law ($n = 2$) and cube-root law ($n = 3$) are often used for fitting the PYS spectra of metals and organic materials, respectively [25,26]. With increasing $h\nu$, photoemission from the metal commences at the threshold energy $h\nu_A^{th} = \varepsilon_{vac}^F$, and by increasing $h\nu$ further, photoemission from the organic film then starts at the energy $h\nu_B^{th} = I$. Therefore, the PYS spectrum shows an onset of photoemission indicated by a kink at $h\nu = \varepsilon_{vac}^F$ in the $Y^{1/2}$ plot and a kink at $h\nu = I$ in the $Y^{1/3}$ plot. The kink in the $Y^{1/3}$ plot indicates a contribution to Y by photoemission from the organic film at higher $h\nu$, whereas Y only contains contributions from photoemission from the metal in the energy range of $h\nu$ from ε_{vac}^F to I. The energy difference between $h\nu_A^{th}$ and $h\nu_B^{th}$ corresponds to E_{HOMO}. Information regarding the organic/metal interface can be obtained by monitoring ε_{vac}^F and E_{HOMO} while systematically increasing the organic film thickness. In this paper, we present PYS studies of three typical organic semiconductor films vacuum deposited on an Au substrate: pentacene/Au, copper phthalocyanine (CuPc)/Au, and perfluorinated zinc phthalocyanine (F_{16}ZnPc)/Au. By comparison of the PYS results obtained herein with previously reported data using UPS, differences between the PYS and UPS results are determined, even for the same system. These differences are closely related to the differences in the experimental principles of the two methods. In particular, PYS may significantly reduce the final state effects of the photoemission, leading to increased accuracy of the energy level diagram of the organic/metal interface.

2. Experimental

The PYS measurement system consists of a UV light source and a current measurement unit (Keithley 6430 source-measure unit). The detailed design of the apparatus has been previously described [21]. The UV light source consists of a deuterium lamp and a monochromator (JASCO SS-10) with a resolution of 3.9 nm (0.04–0.12 eV in the present wavelength region of 200–350 nm). The photon intensity distribution of this light source was measured using a calibrated photodiode (Hamamatsu Photonics S1227–1010BQ). Pentacene and F_{16}ZnPc samples with a quoted purity of ~95% were purchased from Aldrich and were purified by a single vacuum sublimation. A CuPc sample with a quoted purity of >99% was purchased from TCI and was purified by vacuum sublimation once. A clean Au substrate was prepared *in situ* in the PYS chamber by vacuum deposition of a thick Au film on a Si(100) substrate. The organic film was vacuum deposited on the clean Au substrate in the PYS chamber. The deposition rate of the organic film was monitored using a quartz microbalance and adjusted to be approximately 0.01 nm/s for all of the organic samples. During the deposition of the organic film, the substrate was kept at room temperature. After the deposition, the sample was immediately moved to the measurement position without being exposed to air. A voltage of 200 V was applied between the negatively biased sample and the grounded ring-shaped collector electrode placed in front of the sample during the photocurrent measurement [21]. Such a voltage ensures highly efficient collection of the emitted photoelectrons. The photocurrent measured in the PYS on organic sample is typically less than 5×10^{-11} A. This is about 10^{-1} times that of UPS measurement. Therefore, the PYS measurement gives a lot less damage on the organic sample by light irradiation. The acquisition of a single PYS spectrum required approximately 3 min.

3. Results and discussion

3.1. Pentacene/Au interface

Pentacene is well known as a promising material for OFETs due to its relatively high hole mobility [27]. Accordingly, the pentacene/Au interface has generated considerable attention as a model interface for understanding the hole injection properties in OFETs [20,28–31]. In Fig. 3, the data from the PYS spectra of the pentacene film depos-

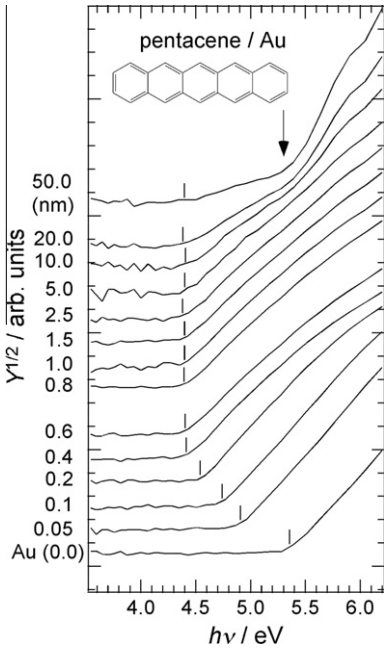

Fig. 3. PYS spectra of pentacene/Au interface. The ordinate and abscissa represent the photoelectron yield, $Y^{1/2}$, and excitation photon energy, $h\nu$, respectively. Each spectrum was obtained with a different thickness of the pentacene film, represented by the numbers next to the left axis. The molecular structure of pentacene is also shown.

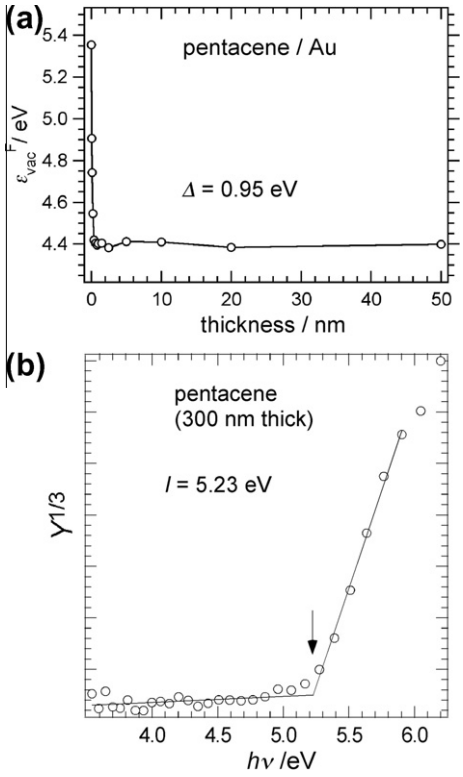

Fig. 4. (a) Film thickness dependence of ε_{vac}^{F} for pentacene/Au interface. (b) PYS spectrum for 300 nm thick pentacene film. $Y^{1/3}$ is plotted against $h\nu$ in order to estimate I of the pentacene film. The onset of $Y^{1/3}$ (indicated with an arrow) gives the threshold energy of $h\nu$, which corresponds to I of the pentacene film.

ited on the Au substrate near the photoelectric threshold energy measured *in situ* are plotted to the 1/2 power against $h\nu$. The $Y^{1/2}$ plot provides information on the photoemission from the Au substrate. Each spectrum in Fig. 3 was obtained with a different thickness of the pentacene film. The pentacene film thickness increases from 0.0 nm (Au) to 50 nm moving up the figure. The vertical bars in the figure indicate the onset of photoemission. In the low $h\nu$ region right above the threshold, only photoelectrons from the Au substrate contribute to the PYS spectra. Therefore, ε_{vac}^{F} can be obtained from the straight portion of the square-root plot. The value of ϕ_{Au} is estimated to be 5.35 eV from the spectrum of the sample with no pentacene film (0.0 nm thickness), where ϕ_{Au} is the work function of Au. This value of ϕ_{Au} indicates the absence of contamination on the Au substrate. Generally, contaminated Au substrates show a ϕ_{Au} value below 5 eV [32]. The data presented in Fig. 3 clearly demonstrate that ε_{vac}^{F} decreases rapidly as the film thickness is incrementally increased from 0.0 to 0.4 nm. However, there is no significant thickness dependence of ε_{vac}^{F} for the films thicker than 0.6 nm. Fig. 4a shows the film thickness dependence of ε_{vac}^{F} derived from the series of spectra presented in Fig. 3. With increasing film thickness, there is a precipitous drop in ε_{vac}^{F} up to the pentacene/Au interface within 0.4 nm thickness, which corresponds roughly to a monolayer of a pentacene film; at film thicknesses higher than 0.6 nm, ε_{vac}^{F} assumes a constant value of around 4.4 eV. The reduction in ε_{vac}^{F} reaches 0.95 eV, which is caused by Δ formation right at the interface. Roughly speaking, the Δ observed on the Au substrate can be interpreted to be the result of the

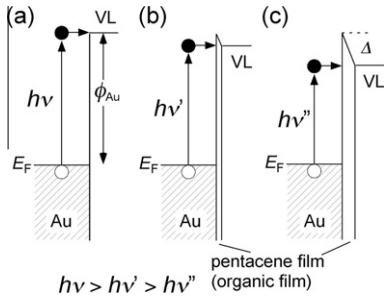

Fig. 5. Schematic drawings of photoemission process in very early stage of deposition of pentacene film. Drawing (a) shows the process for the Au substrate (b) and (c) explain the reduction in $h\nu$ required to generate the photoemission. The electric double layer, Δ is formed by increasing the film thickness of pentacene film up to the monolayer thickness, and the vacuum level (VL) is lowered. Only the VL is shown, and molecular orbitals of pentacene are not shown.

so-called "push-back" effect suggested by Ishii et al. [1], in which the wave functions of the conduction electrons ejected from the metal surface are pushed back into the bulk upon adsorption of the molecules due to Pauli repulsion by the mixing of the wave functions of the metal and the molecule. Such variation in the surface electron density induces an electric dipole at the organic/metal interface

directed toward the organic film in many cases. Fig. 5 depicts the progress of the photoemission from Au during the formation of Δ. As shown in Fig. 5a, the photoemission from the Au substrate without the pentacene film occurs above $h\nu = \phi_{Au}$. The deposition of the pentacene film onto the Au substrate decreases the vacuum level until the monolayer of pentacene is completed due to the progression of Δ, and therefore, the photon energy required for the emission of the photoelectrons decreases from $h\nu'$ to $h\nu''$ (Fig. 5b and c). The reduction in ε^F_{vac} shown in Fig. 4a can be explained accordingly, and ε^F_{vac} no longer decreases after the formation of Δ, as indicated by the plateau in the figure. The PYS spectra of the thicker films (20 nm and 50 nm) in Fig. 3 show kinks around $h\nu = 5.3$ eV (indicated by an arrow), which are caused by photoemission from the pentacene film. For the pentacene films thinner than 10 nm, no photoemission from pentacene is observed in the PYS spectra. By plotting the PYS spectrum in $Y^{1/3}$ for the film thickness of 50.0 nm, E_{HOMO} and I were estimated to be approximately 0.98 and 5.38 eV, respectively. I for the pentacene film with 300 nm thickness was estimated to be 5.23 eV from the PYS spectrum plotted to the 1/3 power against $h\nu$ (Fig. 4b).

The obtained energy level diagram for the pentacene/Au interface is summarized in Fig. 6. The derived hole injection barrier from the Au to the pentacene film, E_{HOMO}, is ~0.98 eV. Based on numerous studies of the pentacene/Au interface by means of UPS, the difference between the results obtained by PYS in this study and the previously reported UPS results was examined. Selected values of ϕ_{Au}, Δ, E_{HOMO}, and I reported using UPS are listed in Table 1 for comparison with the results of PYS obtained herein [20,28–31]. In order to obtain E_{HOMO} and I using UPS, the HOMO energy must be estimated with respect to E_F. All of the cited data for E_{HOMO} and I were obtained using the onset energy of the HOMO peak of the pentacene film in the UPS spectra as the HOMO energy. The method for analyzing the UPS spectra to derive the values of the physical parameters listed in Table 1 is always accompanied with some ambiguities. For example, even a small difference in the determination of the onset energy position of the HOMO peak in the UPS spectrum sometimes brings about a divergence in the values of E_{HOMO} and I among different groups. On the other hand, the determination of these values with PYS is well defined, with better energy resolution, as shown in Figs. 3 and 4b. In addition, a novel mechanism of the photoelectron detection of PYS enables us to apply PYS to insulating materials, and PYS can also be applied to very thick organic films, with thicknesses exceeding several hundred nanometers [22]. Therefore, it is possible to obtain a reliable datum of I for the organic film without the influence of the substrate using PYS. UPS measurements on such thick organic films frequently suffer from charging effects. Nevertheless, the results obtained by PYS and UPS show a level of consistency (Table 1) within experimental error. This indicates that the estimation of the HOMO energy of the organic film using the onset energy of the HOMO peak in the UPS spectrum is confirmed to be an appropriate method. For example, the consistency in the values of I determined by PYS and UPS shows that the onset of the PYS spectrum caused by the photoemission from the pentacene film in Fig. 4b corresponds to the energy interval between the vacuum level and onset of the HOMO peak observed in the UPS spectrum. In general, the HOMO level of the organic film exhibits Gaussian distribution with a certain energy width due to the environmental inhomogeneity of the organic molecules [33]. The HOMO peak in the UPS spectrum is broadened not only because of the experimental energy resolution and thermal effects but also because of the energy distribution of the molecular orbitals. Therefore, the HOMO peak energy, not the onset energy, in the UPS spectra sometimes does not assume definite meaning for the discussion of the optical or transport properties of the organic film.

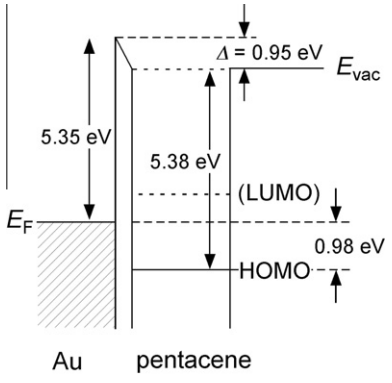

Fig. 6. Schematic energy level diagram for pentacene/Au interface obtained by PYS.

Hereafter, we focus on the difference in Δ. Table 1 indicates that the Δ value reported by Amy et al., Kang et al., and Schoeder et al., appears smaller than that of other reports [20,28,29]. In addition, "band bending" was also observed at the pentacene/Au interface in the aforementioned reports, where the vacuum level and orbital energies gradually decrease by 0.2–0.4 eV with increasing film thickness. In this instance, the term "band bending" does not necessarily refer to the definition of "band bending" used for inorganic semiconductors. The band bending for inorganic semiconductor interfaces is caused by the formation of a depletion layer at the carrier-doped semiconductor/metal interface to achieve thermodynamic equilibrium, although the phenomenon itself is very similar to that for organic/metal interfaces. In many instances, the band bending for organic semiconductor films simply indicates the phenomenon whereby all of the energy levels such as the HOMO, lowest occupied molecular orbital (LUMO), core levels, and vacuum level continuously change upon deposition of the organic film. Because there is a negligible amount of carriers inside the organic film in most cases, especially in the cases of small molecules, the origin of the band bending may be essentially different from that in doped inorganic semiconductors. By taking into account the reduction in ε^F_{vac} caused by band bending (Δ_{BB}) at the pentacene/Au interface, the sum of Δ and Δ_{BB} are 0.95, 1.2, and 0.8 eV for the studies by Amy et al., Kang et al., and Schroeder et al., respectively [20,28,29]. These values of $\Delta + \Delta_{BB}$ are relatively consistent with the Δ value obtained in this study. As suggested by Amy et al., one pos-

Table 1
Comparison of the parameters for pentacene films deposited on the Au substrate, reported by several groups using UPS [20,28–31], with the results obtained using PYS in this study. ϕ_{Au}, Δ, E_{HOMO}, and I represent the work function of the Au substrate, electric double layer, HOMO energy, and ionization energy of the thick pentacene film, respectively. d is the pentacene thickness for the measurement of I. The cited values for E_{HOMO} and I were estimated using the onset energy of the HOMO peak of the pentacene film in the UPS spectra.

	ϕ_{Au}/eV	Δ/eV	E_{HOMO}/eV	I/eV	d/nm
This study (PYS; polycrys. Au)	5.35	0.95	0.98	5.23	300
Schoeder et al. [29] (UPS; Au(1 1 1))	5.47	0.87	0.55	5.07	50
Kang et al. [28] (UPS; polycrys. Au)	5.2	0.76	0.96	4.98	102.4
Koch et al. [30] (UPS; polycrys. Au)	5.4	1.05	0.85	5.2	15
Koch et al. [31] (UPS; Au(1 1 1))	5.50	0.95	0.60	5.15	Monolayer
Amy et al. [20] (UPS; polycrys. Au)	5.05	0.6	0.47	4.49	10

sible origin of the band bending observed in the pentacene/Au interface with UPS is the characteristic final state effect of the photoemission [20]. From a simple view of the photoemission process with sudden approximation, the photoemission probability can be calculated by *Fermi's golden rule*. The photoemission spectrum appears at the energy that satisfies the energy conservation rules, E_f–$E_i = h\nu$, where E_f, E_i, and $h\nu$ are the total energy of the system at the final state, at the initial state of the photoemission process, and excitation photon energy, respectively. E_f includes the relaxation energy of the photohole created upon photoemission. Therefore, the molecular orbital energy, in a similar manner to E_{HOMO} in the UPS spectrum, depends on the relaxation energy. In other words, the molecular orbital energy estimated directly from the UPS spectrum is no longer the well-defined Koopman's binding energy that is valid in the one-electron picture. One of the final state effects is the electric polarization of the ionized molecule by photoemission. Excess charge is created at the ionized molecule by the photoemission: the photohole induces electric polarization of the electronic charge density of the surroundings, and the photohole is stabilized in a positive polaron. Concomitantly, E_{HOMO} observed with UPS decreases because of the polarization energy, producing a reduction in the HOMO–LUMO gap compared to the isolated molecule. As such, the photohole polarization energy is larger than that for other final state effects of the photoemission such as molecular conformational changes to the optimized molecular structure for the ionized species and lattice relaxation. Therefore, the downward shift in binding energy from the pentacene/Au interface to thick pentacene film observed by UPS, referred to as band bending here, is indicative of the decrease in the polarization energy in the bulk of the pentacene film. In general, the polarization energy is larger at the organic/metal interface than in the bulk of the organic film because of image charges induced in the metal. It should be stressed here that no band bending is observed in the pentacene/Au interface using PYS, in contrast to the UPS results. The HOMO of pentacene remains constant throughout the entire thickness range after completion of the monolayer, as shown in Fig. 6. In the final state of UPS process, the photohole at the pentacene molecule forms a positive polaron. In this case, the photohole is localized at a single molecular site and induces electric polarization of the surroundings. On the other hand, the photoelectrons detected in the low $h\nu$ region, right above the threshold of the PYS spectra, originate only from the Au substrate. The photohole created in the Au substrate by photoemission is immediately compensated, and thus, electric polarization effects affect the final states for the photoemission to a much lesser extent; the Δ value derived from the PYS results is highly reliable. Accordingly, there is an underlying fundamental difference in the experimental principles for the observation of Δ using PYS and UPS. It can thus be concluded that the previously reported band bending observed in the pentacene/Au interface using UPS is caused by the electric polarization effect.

As discussed above, the values of $\Delta + \Delta_{BB}$ obtained by UPS analysis of the pentacene/Au interface are relatively consistent with the Δ value obtained using PYS. This fact suggests that Δ_{BB} should be taken into account when UPS is used to estimate the magnitude of the electric dipole layer.

3.2. CuPc/Au interface

The results obtained for the CuPc/Au substrate interface are very similar to those of pentacene/Au. CuPc is a typical organic semiconductor that is frequently used in hole-injection layers at the anode interface in OLEDs and as a donor molecule in the organic photovoltaic cell [34–37]. Fig. 7 shows the PYS spectra of CuPc film deposited on the Au substrate near the photoelectric threshold energy measured *in situ*. The PYS spectra are plotted to the 1/2 power versus $h\nu$. Each spectrum was obtained with a different thickness of the CuPc film. The film thickness of CuPc increases from 0.0 nm (Au) to 20 nm from the bottom to the top of the figure. The vertical bars in the figure indicate the onset of the spectra. In the low $h\nu$ region right above the threshold, only photoelectrons from the Au substrate contribute to the PYS spectra. The film thickness dependence of ε^F_{vac} is shown in Fig. 8a (open circles). Similar to the pentacene/Au case, ε^F_{vac} shows an initial drop in the very thin film region below 0.3 nm and assumes a constant value of around 4.55 eV at increased film thickness (above ~1 nm). The Δ value is estimated to be approximately 0.80 eV from the spectra. The kink (indicated by arrows in Figs. 7 and 8b), which indicates the contribution of photoemission from the CuPc film to the PYS spectra, appears around 5.4 eV above a film thickness of 5.0 nm. On the other hand, as mentioned above, there is not a kink observed in the PYS spectra of the pentacene films thinner than 10 nm. This difference between pentacene and CuPc

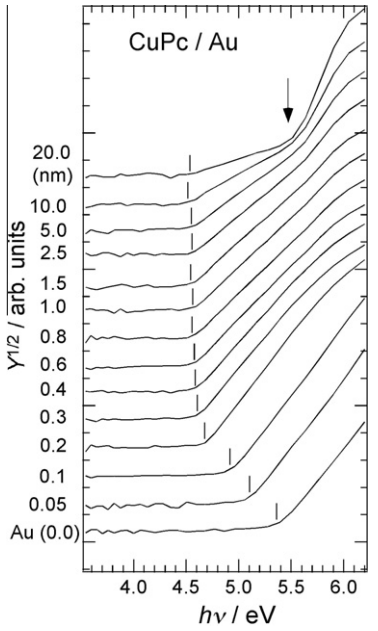

Fig. 7. PYS spectra of CuPc/Au interface. The ordinate and abscissa represent the photoelectron yield, $Y^{1/2}$, and excitation photon energy, $h\nu$, respectively. Each spectrum was obtained with a different thickness of the CuPc film, represented by the numbers next to the left axis.

may be attributed to the difference in film morphology at the early stage of the film growth on Au substrate. It is known that thin pentacene film with several nm thickness on Au substrate consists of pentacene islands [38]. Thus the substrate surface is partly exposed even in the 5 nm thickness pentacene film and the contribution from the Au substrate to the PYS spectra still remains. In contrast to pentacene, a CuPc monolayer on Au substrate is defined as the amount of nearly flat lying CuPc that entirely covers the substrate surface and shows an almost perfectly ordered layer [39]. E_{HOMO} values of the CuPc films with thicknesses of 5.0, 10.0, and 20.0 nm, which were obtained by measuring the energy of the kink with respect to ε^{F}_{vac} in the PYS spectra plotted in $Y^{1/3}$, are also given in Fig. 8a (open squares). E_{HOMO} shows minimal thickness dependence. I for the CuPc films with 100 nm thickness, derived from the PYS spectra plotted to the 1/3 power against $h\nu$ in Fig. 8b, is 5.36 eV. On the other hand, I for the film with 20.0 nm thickness is 5.56 eV. I for the very thick film (100 nm) is smaller than that for the much thinner film (20.0 nm) by 0.2 eV. The small I in the very thick film may be caused by polycrystalline film formation in the thick film. The energy level diagram for the CuPc/Au interface is presented in Fig. 9. The hole injection barrier from the Au to the CuPc film, E_{HOMO}, is ~1.0 eV. The difference in the electronic structure at the CuPc/Au interface derived using UPS versus PYS is considered based on a comparison between the results of this study and a previously reported study by Peisert et al. on the CuPc/Au interface [40], as listed in Table 2. The value of Δ derived from the UPS results in Peisert's report is smaller than the value obtained this study by 0.4 eV. Peisert et al. reported band bending

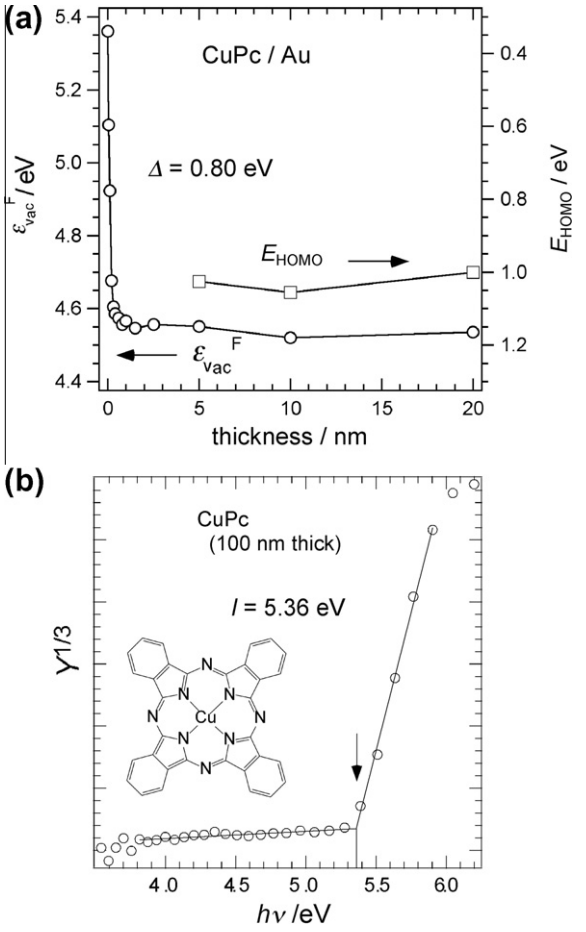

Fig. 8. (a) Film thickness dependence of ε^{F}_{vac} (open circles) and E_{HOMO} of the films with thicknesses of 5.0, 10.0, and 20.0 nm (open squares) for CuPc/Au interface. (b) PYS spectrum for 100 nm thick CuPc film. $Y^{1/3}$ is plotted against $h\nu$ in order to estimate I of the CuPc film. The onset of $Y^{1/3}$ (indicated with an arrow) gives the threshold energy of $h\nu$, that corresponds to I of the CuPc film. The molecular structure of CuPc is also shown.

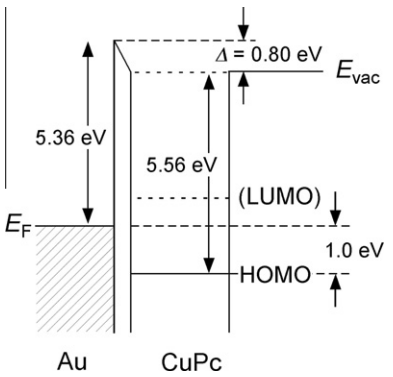

Fig. 9. Schematic energy level diagram for CuPc/Au interface obtained by PYS.

from a CuPc layer thickness of less than 2 nm to over 9 nm thickness, and they discussed it in terms of the

Table 2
Comparison of parameters for CuPc films deposited on the Au substrate reported by Peisert et al. [40] using UPS with those obtained in this study using PYS. ϕ_{Au}, Δ, E_{HOMO}, and I represent the work function of the Au substrate, electric double layer, HOMO energy, and ionization energy of thick CuPc film, respectively. d is the CuPc thickness for the measurement of I. The cited values for E_{HOMO} and I were estimated using the onset energy of HOMO peak of CuPc film in UPS spectra.

	ϕ_{Au}/eV	Δ/eV	E_{HOMO}/eV	I/eV	d/nm
This study (PYS; polycrys. Au)	5.36	0.80	1.0	5.36	100
Peisert et al. [40] (UPS; polycrys. Au)	5.3	1.2	0.9	5.0	9.2

charge transfer from CuPc to Au to achieve Fermi level alignment [40] As depicted in Fig. 9, the PYS results show that ε^F_{vac} remains nearly constant up to a CuPc thickness of 20 nm, contrary to their report. This clearly shows that the band bending observed at the CuPc/Au interface using UPS is attributed to the hole polarization effect as a characteristic final state effect of photoemission, as previously discussed for pentacene/Au. The electron transfer from a Sm substrate to a CuPc film at the CuPc/Sm interface was reported by Tanaka et al., which generated a negative value of Δ [14]. They also reported that there is no band bending above a CuPc film thickness of approximately 2 nm. This implies that the charges transferred from the substrate to the organic film generate the negative Δ, but do not necessarily induce band bending in the organic film. The magnitude of $\Delta + \Delta_{BB}$ observed in the C 1s core level energy by Peisert et al. is approximately 0.8 eV, which is in good agreement with the value of Δ obtained using PYS [40].

Band bending at the CuPc/graphite interface, observed using UPS, was discussed by Yamane et al. in terms of the molecular orientation depending on the film thickness [41]. CuPc molecules are flat and lay directly on the graphite substrate; for thick films, the molecules gradually tilt as the film thickness increases. It was suggested in that study that although CuPc does not have a permanent dipole, electric dipoles are induced by a gradient of the intermolecular interaction along the surface normal due to the continuous increase in the molecular tilt angle with the film thickness, which might explain the observed band bending in the CuPc/graphite interface. Additionally, in the case of CuPc/Au, Tokito et al. reported a similar continuous change in the molecular orientation of CuPc with increasing film thickness [42]. The flat CuPc molecules lay directly on the Au substrate, and the molecules are gradually tilted as the film thickness increases, similar to the CuPc/graphite interface. This gradual orientation change of the CuPc molecular plane should correspond to the formation of a polycrystalline film with increased film thickness [40]. However, the results of the current study using PYS clearly indicate that there is no band bending at the CuPc/Au interface. We conclude that the continuous change in the molecular orientation of CuPc does not induce the electric dipoles inside the film, at least in the case of CuPc/Au. It is reasonable to attribute the band bending observed at the CuPc/Au interface to the final state effect of photoemission.

3.3. F_{16}ZnPc/Au interface

Fig. 10 shows the PYS spectra measured *in situ* for the F_{16}ZnPc film deposited on the Au substrate. The spectra near the photoelectric threshold energy are plotted to the 1/2 power versus $h\nu$. Due to its very high electron affinity (E_A), F_{16}ZnPc is a prime candidate as a stable *n*-type material for OFETs [43,44]. The perfluorination of zinc phthalocyanine (ZnPc) greatly stabilizes the molecular orbitals of ZnPc. On the other hand, the HOMO–LUMO gap is affected to a lesser extent by perfluorination; consequently, E_A is dramatically enhanced by the decrease in the LUMO energy. The thickness of the F_{16}ZnPc film was varied for each spectrum in Fig. 10, with the thickness increasing from 0.0 nm (Au) to 10.0 nm moving up the figure. The vertical bars in the figure indicate the onset of the spectra. In the low $h\nu$ region right above the threshold, only photoelectrons from the Au substrate contribute to the PYS spectra. In contrast to pentacene/Au and CuPc/Au, no kink was observed in the PYS spectrum for the thicker F_{16}ZnPc films due to the very high I value of F_{16}ZnPc (I = 6.4 eV) [45]. The film thickness dependence of ε^F_{vac} is shown in Fig. 11. ε^F_{vac} declines in the region with very thin film thickness of below 0.5 nm, and Δ is estimated to be approximately 0.36 eV. The value of Δ for F_{16}ZnPc/Au is much smaller than that of pentacene/Au and CuPc/Au. Because a small difference is expected between CuPc and ZnPc in terms

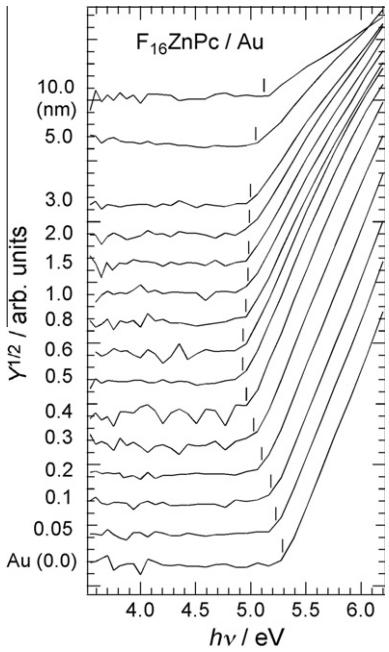

Fig. 10. PYS spectra of F_{16}ZnPc/Au interface. The ordinate and abscissa represent photoelectron yield, $Y^{1/2}$, and excitation photon energy, $h\nu$, respectively. Each spectrum was obtained with different thickness of the F_{16}ZnPc film, represented by the numbers next to the left axis.

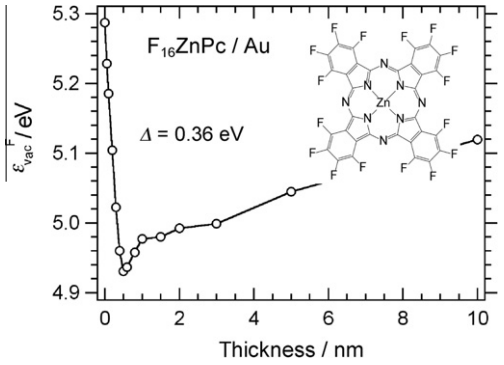

Fig. 11. Film thickness dependence of ε_{vac}^{F} for F_{16}ZnPc /Au interface. The molecular structure of F_{16}ZnPc is also shown.

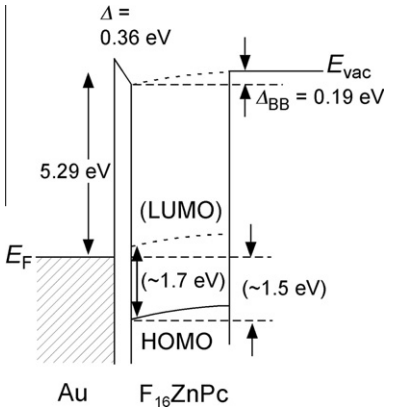

Fig. 12. Schematic energy level diagram for F_{16}ZnPc/Au interface obtained by PYS. The value of E_{HOMO} right at the interface (~1.5 eV) and the HOMO–LUMO gap (~1.7 eV) are cited from literature [45,53].

of the electronic structure around E_F and the effect of fluorination of the molecule, it is meaningful to refer to the reported results for CuPc and fluorinated CuPc (F_xCuPc). It was reported that Δ for the fluorinated F_xCuPc/Au interface decreases with the degree of fluorination (x), indicating that the fluorination of the molecule might reduce Δ due to the enhancement of E_A [46]. However, the relationship between the fluorination and a small Δ still remains unclear. Gerlach et al. reported the symmetry breaking of the F_{16}CuPc molecule adsorbed on Cu(1 1 1) or Ag(1 1 1) using an X-ray standing wave technique (XSW) [47]. They showed that the carbon–fluorine (C–F) bonds of F_{16}CuPc chemisorbed onto Cu and Ag bend toward the opposite side of the substrate. Such non-planar adsorption of the molecule might induce electric dipoles that are oriented toward the metal surface because of the highly electronegative fluorine atoms. The electric dipole layer formed at the interface by the chemisorption of F_{16}CuPc thus increases the surface potential. As a result, Δ of the fluorinated adsorbate is reduced to a higher degree on Cu and Ag substrates than that of the non-fluorinated molecules. Very similar phenomena were reported for the planar molecule perylentetracarbonsäuredianhydrid (PTCDA) on Ag substrates [48,49]. The carbon–oxygen bonds in PTCDA bend, and the PTCDA shows a non-planar adsorption on Cu and Ag substrates. Thus, chemisorbed PTCDA also possesses induced electric dipoles [48]. However, this explanation of the variation in Δ as a consequence of induced dipoles in the chemisorbed molecule does not appear plausible in the case of F_{16}ZnPc/Au because it is unlikely that F_{16}ZnPc is chemisorbed on the Au substrate. Charge transfer or hybridization of the wave functions between F_{16}ZnPc and the Au substrate is expected to be a low probability event because of the inertness of Au. In fact, de Oteyza et al. reported that F_{16}ZnPc adsorbed on Au(1 1 1) has a much larger adsorption distance compared to Cu(1 1 1) or Ag(1 1 1) and the molecule retains its planar structure [50]. This is also true for PTCDA/Au [48]. The comparison between pentacene/Au(1 1 1) and perfluorinated pentacene (PFP)/Au(1 1 1) carried out by Koch et al. indicates that the smaller Δ value observed for PFP/Au(1 1 1) compared to pentacene/Au(1 1 1) originates from a larger adsorption distance of PFP than pentacene, given that the adsorption distance strongly influences Δ in a simple "push-back" scenario [31,51]. However, from the report by de Oteyza et al., there is not much difference in the adsorption distance of CuPc versus F_{16}CuPc on Au(1 1 1), indicating that fluorination does not affect the adsorption distance [52,53]. The theoretical examination of the influence of fluorination of the phthalocyanines on Δ is required as the next step.

As seen in Fig. 11, ε_{vac}^{F} for film thicknesses above 0.5 nm exhibits a conspicuously different thickness dependence from the pentacene/Au and CuPc/Au interfaces. ε_{vac}^{F} increases gradually with the thickness of the F_{16}ZnPc film. The schematic energy level diagram for F_{16}ZnPc/Au is shown in Fig. 12. The reported value of the HOMO–LUMO gap of F_{16}ZnPc is approximately 1.7 eV [53], and thus, the LUMO of the F_{16}ZnPc film is very close to the Fermi level right at the interface, which satisfactorily explains the n-type electrical properties of the F_{16}ZnPc film [43,44]. This result is in good agreement with that of a previous study, which shows that a similar upward band bending was observed using UPS [45]. The energy shift caused by band bending (Δ_{BB}) is approximately 0.19 eV up to a film thickness of 10 nm, which is consistent with the UPS result. In contrast to pentacene/Au and CuPc/Au, the fact that band bending, which occurs for a film thickness of over 10 nm, is observed using both PYS and UPS clearly indicates that the band bending observed at the F_{16}ZnPc/Au interface is not caused by the final state effects of photoemission. The surface potential is genuinely raised as the thickness of F_{16}ZnPc increases, and band bending actually occurs at the F_{16}ZnPc/Au interface. Band bending, including the reduction in Δ at the F_{16}CuPc/Au interface, was also discussed in terms of the thermodynamic equilibrium achievement, which gives Fermi level alignment by Peisert et al. [46]. However, the question of whether it was possible to apply the classical picture to the organic semiconductor film still remains controversial. It has been postulated that in many organic semiconductors, the carrier is a small polaron and the transport mechanism is discussed based on the hopping model. This situation is quite different from inorganic semiconductors where the transport properties can be well explained based on the coherent energy band-conduction mechanism.

It should be noted that Hwang et al., reported that the charge accumulated layer formed at the interface between the conductive polymer films and metal substrates induces band bending [54]. The resulting filed generated the excess charges at the interface shifts the polymer levels to limit charge penetration in the bulk of the film. On the other hand, Sueyoshi et al. [55,56], and Mao et al. [57], provides the discussion about the energy level alignments at the organic/metal interface based on the low density gap-states which reside in the HOMO–LUMO gap only at the interface. The gap-states are caused as the results of the structural disorder at the organic/metal interface. These models are associated with the origins of the Schottky barrier at the conventional inorganic semiconductors interfaces. It is well known that for III–V compound semiconductors, the Schottly barrier is formed due to defects near the interface. The surface Fermi level of the compounds is pinned at the certain energy by induced gap-states by the defects.

Another possibility for the upward band bending at the F_{16}ZnPc/Au interface is the existence of negatively ionized impurities, unintentionally doped in the F_{16}ZnPc film. It is known that in some organic films, band bending is dramatically affected by very small amounts of acceptor or donor molecules introduced by intentional doping [12,13,45,58]. For example, the titanyl phthalocyanine (TiOPc) film deposited in ultrahigh vacuum (UHV) shows downward band bending, whereas the TiOPc film deposited under an oxygen atmosphere (the partial pressure of O_2 of 1.3×10^{-2} Pa) shows upward band bending [12]. This difference in the band bending between the films deposited under different conditions has been interpreted as follows: there are unintentionally doped impurity cations that produce the downward band bending in the film deposited in UHV, and negatively ionized oxygen produces an upward band bending in the film deposited in the oxygen atmosphere. The amount of the doped oxygen should exceed that of unintentionally doped cation impurities. The number of unintentionally doped impurities in the TiOPc film is, nevertheless, very small, which was estimated at $\sim 3.4 \times 10^{17}$ cm^{-3} by using a solution of the Poisson equation with constant space-charge density [12]. It is very difficult to probe the impurity directly by means of spectroscopic techniques such as UPS, and thus, the impurities have not yet been experimentally identified.

On the other hand, the use of the near-edge X-ray absorption fine structure technique and infrared reflection absorption spectroscopy studies on F_{16}ZnPc/Au and F_{16}ZnPc revealed that the nearly flat molecular orientation of F_{16}ZnPc gradually changes to random or tilting orientation with increasing thickness of F_{16}ZnPc [59]. This indicates that the intermolecular interactions within the F_{16}ZnPc film depend on the film thickness. The discussion of CuPc/graphite by Yamane et al. [41] indicated that such a thickness-dependent intermolecular interaction might be one of the possible origins of the band bending at the F_{16}ZnPc/Au interface. However, an account of the difference between F_{16}ZnPc/Au and CuPc/Au is still necessary because CuPc/Au also shows thickness dependence of the molecular orientation but no band bending.

4. Conclusions

We have shown that PYS is a powerful tool for probing organic/metal interfaces due to its long probing depth. PYS offers the particular advantage of precise measurement of the carrier injection barrier at the organic/metal interface. The organic film thickness dependence of the PYS spectrum for the metal substrate covered with an organic film provides reliable information about Δ and significantly minimizes the effects of the characteristic final state effect, known as the electric polarization effect, on band bending phenomena relative to UPS.

The PYS results show that no band bending was observed at pentacene/Au and CuPc/Au interfaces, whereas band bending was reported in previous studies employing UPS [28,29,40]. The origin of the band bending in these films has been discussed only occasionally so far. However, the comparison of the results obtained using PYS and UPS clearly shows that the band bending observed by UPS is caused by the electric polarization effect [20]. It can be concluded that caution should be exercised when using UPS results to interpret the electronic structure at the organic/metal interface. On the other hand, band bending at the F_{16}ZnPc/Au interface was observed using both PYS and UPS, in contrast to the pentacene/Au and CuPc/Au interfaces [46]. There is, in fact, a thickness dependence of ε_{vac}^{F} in the F_{16}ZnPc film. One possible origin of the band bending is the existence of gap-states at the interface that accommodate excess charges and thermal equilibrium is achieved. Another possibility of the band bending is the existence of unintentionally doped impurities. Although the effects of the fluorination of the molecule on the interface electronic structure remain obscure, some reports on intentional carrier doping of organic semiconductor films demonstrated the possibility of the existence of ionized impurities within the F_{16}ZnPc film. Because it has generally been believed that band bending also has a significant influence on the carrier injection properties at the organic/metal interface, a re-examination of the various organic/metal interfaces by comparing the PYS and UPS results is warranted.

Acknowledgments

This study was supported in part by a Grant-in-Aid for Scientific Research (S) (Grant No. 19105005) from the Ministry of Education, Culture, Sports, Science and Technology of Japan (MEXT) and Special Coordination Funds for Promoting Science and Technology from MEXT.

References

[1] H. Ishii, K. Sugiyama, E. Ito, K. Seki, Adv. Mater. 11 (1999) 605.
[2] H. Ishii, K. Seki, in: W.R. Salaneck, K. Seki, A. Kahn, J.J. Pireaux (Eds.), Conjugated Polymer and Molecular Interfaces, Marcel Dekker, New York, 2002, p. 293.
[3] H. Vázquez, R. Oszwaldowski, P. Pou, J. Ortega, R. Pérez, F. Flores, A. Kahn, Europhys. Lett. 65 (2004) 802.
[4] H. Vázquez, W. Gao, F. Flores, A. Kahn, Phys. Rev. B 71 (2005) 041306.
[5] J.X. Tang, C.S. Lee, S.T. Lee, Appl. Phys. Lett. 87 (2005) 252110.
[6] Y.C. Zhou, J.X. Tang, Z.T. Liu, C.S. Lee, S.T. Lee, Appl. Phys. Lett. 93 (2008) 093502.
[7] W. Mönch, Appl. Phys. Lett. 88 (2006) 112116.

[8] C. Tengstedt, W. Osikowicz, W.R. Salaneck, I.D. Parker, C.-H. Hsu, M. Fahlman, Appl. Phys. Lett. 88 (2006) 053502.
[9] M. Fahlman, A. Crispin, X. Crispin, S.K.M. Henze, M.P. de Jong, W. Osikowicz, C. Tengstedt, W.R. Salaneck, J. Phys.: Condens. Matter 19 (2007) 183202.
[10] H. Fukagawa, S. Kera, T. Kataoka, S. Hosoumi, Y. Watanabe, K. Kudo, N. Ueno, Adv. Mater. 19 (2007) 665.
[11] N. Koch, A. Vollmer, Appl. Phys. Lett. 89 (2006) 162107.
[12] T. Nishi, K. Kanai, Y. Ouchi, M.R. Willis, K. Seki, Chem. Phys. 325 (2006) 121.
[13] Y. Tanaka, K. Kanai, Y. Ouchi, K. Seki, Chem. Phys. Lett. 441 (2007) 63.
[14] Y. Tanaka, K. Kanai, Y. Ouchi, K. Seki, Org. Electr. 10 (2009) 990.
[15] E. Ito, H. Oji, N. Hayashi, H. Ishii, Y. Ouchi, K. Seki, Appl. Surf. Sci. 175–176 (2001) 407.
[16] S. Hüfner, in: Photoelectron Spectroscopy: Principles and Applications, Springer, 2003.
[17] W.R. Salaneck, Phys. Rev. Lett. 40 (1978) 60.
[18] I.G. Hill, A.J. Makinen, Z.H. Kafafi, J. Appl. Phys. 88 (2000) 889.
[19] E.V. Tsiper, Z.G. Soos, W. Gao, A. Kahn, Chem. Phys. Lett. 360 (2002) 47.
[20] F. Amy, C. Chan, A. Kahn, Org. Electr. 6 (2005) 85.
[21] M. Honda, K. Kanai, K. Komatsu, Y. Ouchi, H. Ishii, K. Seki, J. Appl. Phys. 102 (2007) 103704.
[22] Y. Nakayama, S. Machida, T. Minari, K. Tsukagishi, Y. Noguchi, H. Ishii, Appl. Phys. Lett. 93 (2008) 173305.
[23] E.O. Kane, Phys. Rev. 127 (1962) 131.
[24] G.W. Gobeli, F.G. Allen, Phys. Rev. 127 (1962) 141.
[25] J.M. Ballantyne, Phys. Rev. B 6 (1972) 1436.
[26] M. Kochi, Y. Harada, T. Hirooka, H. Inokuchi, Bull. Chem. Soc. Jpn. 43 (1970) 2690.
[27] G. Horowitz, Adv. Mater. 10 (1998) 365.
[28] S.J. Kang, Y. Yi, C.Y. Kim, S.W. Cho, M. Noh, K. Jeong, C.N. Whang, Synth. Met. 156 (2006) 32.
[29] P.G. Schroeder, C.B. France, J.B. Park, B.A. Parkinson, J. Appl. Phys. 91 (2002) 3010.
[30] N. Koch, J. Ghijsen, A. Elschner, R.L. Johnson, J.-J. Pireaux, J. Schwarz, A. Kahn, Appl. Phys. Lett. 82 (2003) 70.
[31] N. Koch, A. Vollmer, S. Duhm, Y. Sakamoto, T. Suzuki, Adv. Mater. 19 (2007) 112.
[32] A. Wan, J. Hwang, F. Amy, A. Kahn, Org. Electr. 6 (2005) 47.
[33] M. Schwoerer, H.C. Wolf, in: Organic Molecular Solids, Chapter 8, Wiley-VCH, 2007, p. 293.
[34] S.M. Tadayyon, H.M. Grandin, K. Griffiths, P.R. Norton, H. Aziz, Z.D. Popovic, Org. Electr. 5 (2004) 157.
[35] P. Peumans, S.R. Forrest, Appl. Phys. Lett. 126 (2001) 79.
[36] Z.R. Hong, Z.H. Huang, X.T. Zeng, Chem. Phys. Lett. 425 (2006) 62.
[37] K. Akaike, A. Opitz, J. Wagner, W. Brütting, K. Kanai, Y. Ouchi, K. Seki, Org. Electron 11 (2010) 1853.
[38] D. Käfer, L. Ruppel, G. Witte, Phys. Rev. B 75 (2007) 085309.
[39] I. Chizhov, G. Scoles, A. Kahn, Langmuir 16 (2000) 4358.
[40] H. Peisert, M. Knupfer, T. Schwieger, J.M. Auerhammer, M.S. Golden, J. Fink, J. Appl. Phys. 91 (2002) 4872.
[41] H. Yamane, Y. Yabuuchi, H. Fukagawa, S. Kera, K.K. Okudaira, N. Ueno, J. Appl. Phys. 99 (2006) 093705-1.
[42] S. Tokito, K. Noda, Y. Taga, J. Phys. D 29 (1996) 2750;
S. Tokito, J. Sakata, Y. Taga, Thin Solid Films 256 (1995) 182.
[43] J. Wang, H. Wang, X. Yan, H. Huang, D. Yan, Chem. Phys. Lett. 407 (2005) 87.
[44] Q. Tang, H. Li, Y. Liu, W. Hu, J. Am. Chem. Soc. 128 (2006) 14634.
[45] S. Tanaka, K. Kanai, E. Kawabe, T. Iwahashi, T. Nishi, Y. Ouchi, K. Seki, Jpn. J. Appl. Phys. 44 (2005) 3760.
[46] H. Peisert, M. Knupfer, T. Schwieger, G.G. Fuentes, D. Olligs, J. Fink, Th. Schmidt, J. Appl. Phys. 93 (2003) 9683.
[47] A. Gerlach, F. Schreiber, S. Sellner, H. Dosch, I.A. Vartanyants, B.C.C. Cowie, T.-L. Lee, J. Zegenhagen, Phys. Rev. B 71 (2005) 205425.
[48] S.K.M. Henzea, O. Bauerb, T.-L. Lee, M. Sokolowskib, F.S. Tautza, Surf. Sci. 601 (2007) 1566.
[49] A. Gerlach, S. Sellner, F. Schreiber, N. Koch, J. Zegenhagen, Phys. Rev. B 75 (2007) 045401.
[50] D.G. de Oteyza, A. El-Sayed, J.M. Garcia-Lastra, E. Goiri, T.N. Krauss, A. Turak, E. Barrena, H. Dosch, J. Zegenhagen, A. Rubio, Y. Wakayama, J.E. Ortega, J. Chem. Phys. 133 (2010) 214703.
[51] Y. Morikawa, H. Ishii, K. Seki, Phys. Rev. B 69 (2004) 041403(R).
[52] I. Kröger, B. Standtmüller, C. Kleimann, P. Rajput, C. Kumpf, Phys. Rev. B 83 (2011) 195414.
[53] S. Hiller, D. Schlettwein, N.R. Armstrong, D. Wöhrle, J. Mater. Chem. 8 (1998) 945.
[54] J. Hwang, E. Kim, J. Liu, J. Brédas, A. Duggal, A. Kahn, J. Phys. Chem. C 111 (2007) 1378.
[55] H.Y. Mao, F. Bussolotti, D. Qi, R. Wang, S. Kera, N. Ueno, A.T.S. Wee, W. Chen, Org. Electr. 12 (2011) 534.
[56] T. Sueyoshi, H. Kakuta, M. Ono, K. Sakamoto, S. Kera, N. Ueno, Appl. Phys. Lett. 96 (2010) 093303.
[57] T. Sueyoshi, H. Fukagawa, M. Ono, S. Kera, N. Ueno, Appl. Phys. Lett. 95 (2009) 183303.
[58] C. Chan, W. Gao, A. Kahn, J. Vac. Sci. Technol. A 22 (2004) 1488.
[59] T. Ikame, K. Kanai, Y. Ouchi, E. Ito, A. Fujimori, K. Seki, Chem. Phys. Lett. 413 (2005) 373.